

Conference Article

## Modeling Stress-Strain State in Butt-Welded Joints after TIG Welding

V. Atroshenko, R. Nikiforov and O. Kolenchenko

Ufa State Aviation Technical University, Ufa, Russian Federation

Received 3 September 2015; Accepted 10 September 2015

### Abstract

In this paper mathematical model was developed for definition of thermal-welding cycle influence on welding deformations distribution in flat samples of austenitic steels after TIG welding and developed recommendations to reduce the welding deformation on the machinery for welding with a copper backing.

*Keywords:* TIG welding, residual deformation, finite element method (FEM), the stress-strain state of the construction, the longitudinal and transverse shrinkage.

### 1. Introduction

Automatic tungsten inert gas welding (TIG) is widely used in engine manufacturing for welding thin sheets of corrosion-resistant austenitic steels, most of which welds are produced without filler wire on copper backing in accordance to GOST 14771-76 [1].

The amount of welding input heat and heat transfer to the copper backing bar affects the distribution of residual strains in addition to design features of the machinery for welding and fixture conditions of the parts.

The analytical methods traditionally used to calculate residual strains, allows the approximate calculation of the deformation of welded structures while not taking into account the effect of the fixing arrangements and the value of welding input heat to the copper backing for welding thin sheet structures without additional experimental work.

Thus the development of numerical models to estimate the stress-strain state of welded parts will enable the calculation of the final deformed parts while still in the design stage without further iterations.

### 2. Numerical modeling of residual strains

The distribution of residual strains is obtained by solving the thermal deformation problem with the finite element package ANSYS Multiphysics ver. 14. The solution of the thermal (transient) and the mechanical (stress-strain transient) analyses was separate. In this case the thermal problem elements were transformed into a mechanical type of elements in the second step with the ANSYS procedures.

The calculation of thermal deformation was based on the deformation theory of non-isothermal flow using the parametric design language APDL. Residual stresses in

welded joints of stainless steels do not usually exceed the yield strength and the Baushinger effect has to be taken into account [5]. The model developed to calculate the plastic behavior due to bilinear kinematic hardening (BKIN) has been described in detailed previously [7], while the material deforms following the criteria of von Mises yield [5].

Weld geometry details using a combination of linear and 2D Gauss heat sources. Boundary conditions of convective, contact and emissive heat transfer, the mode of input heat sources and the distribution of effective power between heat sources are described in detail in [2]. For the thermal analysis a three-dimensional 20-node element SOLID 90 was used that supports thermal contact. Conductivity of the contact pair "part-copper backing" was considered as the sum of the thermal conductivities of the air gap between asperities of the contacting materials –  $\alpha^{\text{air}}$  and metal contact –  $\alpha^{\text{met}}$  based on the method of calculating the contact thermal conductivity [2], [3].

To describe the distribution of temperature field  $T(x,y,z,t)$  in a flat sample the differential nonlinear equation of thermal conductivity was used:

$$c\rho \frac{\partial T}{\partial t} = \frac{\partial}{\partial x} \left( \lambda_x \frac{\partial T}{\partial x} \right) + \frac{\partial}{\partial y} \left( \lambda_y \frac{\partial T}{\partial y} \right) + \frac{\partial}{\partial z} \left( \lambda_z \frac{\partial T}{\partial z} \right) \quad (1)$$

where  $\rho(T)$  – density,  $\text{kg/m}^3$ ;  $\lambda(T)$  – thermal conductivity,  $\text{W/(m}\cdot\text{°C)}$ ;  $c\rho$  – heat capacity,  $\text{J/(m}^3\cdot\text{°C)}$ .

The computer model was split in 3 stages which resemble as close as possible the conditions of welding: stage 1 (Loadstep 1) applies to the fixed model a movable heat source; stage 2 (Loadstep 2) calculates the cooling plates following welding and forms the temporarily longitudinal and transverse shrinkage welded plate ( $t = 30$  s); and in the third stage (Loadstep 3) the plate is released from fixture and the longitudinal and transverse shrinkage  $\Delta_{\text{tran}}$  reaches its maximum value ( $t = 10$  s).

Experimental verification of the numerical model was carried out on plates of thin sheet corrosion-resistant austenitic steel 316L measuring  $100 \times 50$  mm with a

\* E-mail address: [otsp\\_ugatu@mail.ru](mailto:otsp_ugatu@mail.ru)

thickness of 1.5; 2.0 and 3.0 mm. Numerical modeling of residual strains was carried out for the welding conditions corresponding to the minimum and maximum input heat  $Q_{th}$  for the following thicknesses: 1,5 mm –  $Q_{th}=111-156$  kJ/m; 2,0 mm –  $Q_{th}=156-234$  kJ/m; 3,0 mm –  $Q_{th}=274-383$  kJ/m. When welding with maximum heat input the influence of the width of the groove in the copper backing on the distribution of residual strains in the weld zone for plates 1.5 to 3.0 mm thick and a width of the groove in the copper backing at  $a = 6$  and 8 mm was determined.

**3. Verification of numerical model and modeling results discussion**

For the purpose of experiments a commercial welding machine was used for welding thin sheets, employing copper backing and a fixing clamp. The pressure of the fixing clamps on the welded plate was 0.6 MPa. For welding in all cases tungsten electrodes WL-20 3 mm in diameter at an angle of 30° were used.

Before each weld operation on the sample applied marks (shown in Fig.1, a). Transverse movement of marks was measured using a tool microscope "BMI-1C" with divisions of ± 5 microns. Location of marks on the sample and on the finite element mesh 3D-model as shown in Fig. 1.

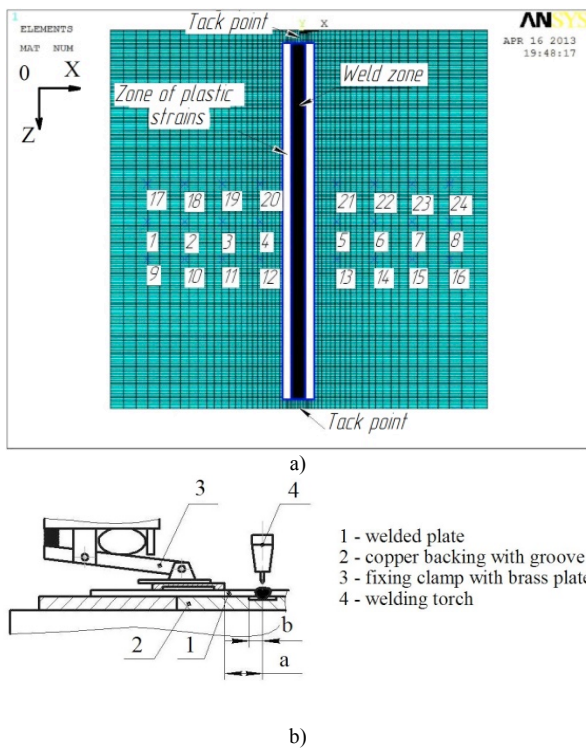


**Fig. 1.** Distribution of marks on the sample after TIG welding (a) and fixing arrangement for the flat sample for welding (b)

The comparison between experimental values of angular distortion, transverse and longitudinal shrinkage and those of numerical modeling are shown in Table. 1. Angular distortion of welded plates and transverse shrinkage were determined from the displacement of nodes of the 3D-model in the axes OY and OX, respectively while the longitudinal shrinkage was determined by the movement of the nodes of the 3D model on OZ and compared to those calculated with traditional analytical equations [4].

**Table 1.** Comparison of the results of numerical modeling and experiment

The angular distortion $\beta$ of the welded plate on the axis OY						
The thickness of the plate, mm	1,5		2,0		3,0	
The welding speed, m/h	18	27	16	25	14	20
$\beta$ in the model, °	0,62	0,73	1,40	0,98	1,70	1,17
$\beta$ on the results of experiments, °	0,78	0,72	1,30	1,20	1,82	1,30
Longitudinal shrinkage of the welded plate along the axis OZ						
$\Delta_{lon}$ from model, mm	0,29	0,20	0,28	0,18	0,26	0,21
$\Delta_{lon}$ from analytical solution [4], mm	0,33	0,24	0,34	0,23	0,37	0,29
	5	0	0	0	3	0
Transverse shrinkage of the welded plate along the axis OX						
$\Delta_{tr}$ in the model, mm	0,47	0,34	0,43	0,32	0,55	0,38
$\Delta_{tr}$ on the results of experiments, mm	0,48	0,36	0,42	0,37	0,61	0,43

The distribution of the relative movement of nodes along OX corresponds to the transverse shrinkage of the welded plate and angular distortion of flat specimens with a thickness of 3.0 mm after TIG welding (Fig. 2). The contour line shows the original shape of the plate before welding.

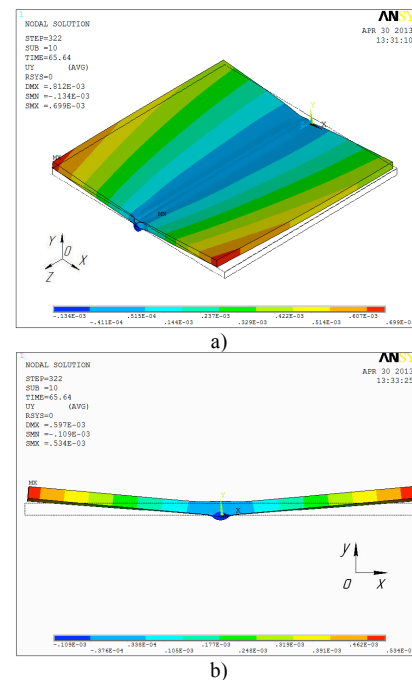


**Fig. 2.** Distribution of relative movement of nodes along the axis OX (a) and angular distortion  $\beta$  of the welded plate (b). Scale factor x8

In order to obtain the quantitative dependencies of the transverse and longitudinal shrinkage for the material thicknesses studied specimens (Table. 2) for the range of parameters of TIG welding employed according to GOST 14771-76 [1] a linear approximation in the package MathCad was used.

In order to study the effect of the location of the clamps

relative to the axis weld and the pressure used on the longitudinal shrinkage a validation of the numerical model of thermal deformation when welding with pressure clamps of 0.3 and 1 MPa, was performed to ensure no slip conditions during welding and leaving it to cool in the

**Table 2.** Quantitative relationship of transverse and longitudinal shrinkage with input heat during welding

The thickness of the plate, mm	Transverse shrinkage $\Delta_{tr}$ , mm		Longitudinal shrinkage $\Delta_{lon}$ , mm	
	$l_{eg}^* = 2$ mm	$l_{eg}^* = 3$ mm	$l_{eg}^* = 2$ mm	$l_{eg}^* = 3$ mm
1,5	$0,068 + 5,991 \cdot 10^{-7} \cdot \frac{Q_{th}}{Q_{th}}$	$0,065 + 6,341 \cdot 10^{-7} \cdot \frac{Q_{th}}{Q_{th}}$	$-9,169 \cdot 10^{-3} + 1,235 \cdot 10^{-6} \cdot \frac{Q_{th}}{Q_{th}}$	$-0,026 + 1,327 \cdot 10^{-6} \cdot \frac{Q_{th}}{Q_{th}}$
2,0	$-0,063 + 8,404 \cdot 10^{-7} \cdot \frac{Q_{th}}{Q_{th}}$	$-0,07 + 8,425 \cdot 10^{-7} \cdot \frac{Q_{th}}{Q_{th}}$	$-0,056 + 8,218 \cdot 10^{-7} \cdot \frac{Q_{th}}{Q_{th}}$	$-0,07 + 8,425 \cdot 10^{-7} \cdot \frac{Q_{th}}{Q_{th}}$
3,0	$-0,019 + 1,34 \cdot 10^{-6} \cdot \frac{Q_{th}}{Q_{th}}$	$-1,101 + 10^{-6} \cdot \frac{Q_{th}}{Q_{th}}$	$-0,045 + 2,25 \cdot 10^{-6} \cdot \frac{Q_{th}}{Q_{th}}$	$-0,014 + 1,964 \cdot 10^{-6} \cdot \frac{Q_{th}}{Q_{th}}$

where  $l_{eg}^*$  – the length of the electrode gap, mm

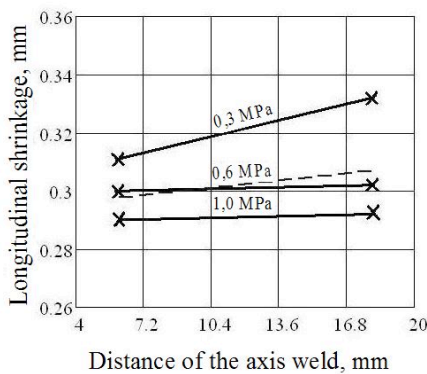


**Fig. 3.** Longitudinal shrinkage dependence on the location of clamps and pressure on the welded plate with thickness of 1.5 mm

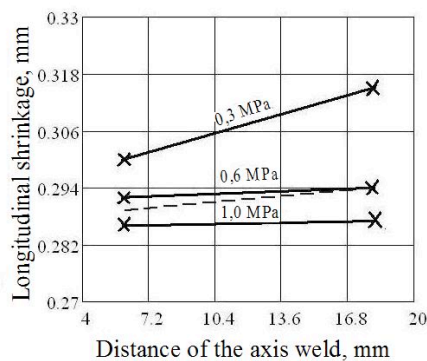


**Fig. 4.** Longitudinal shrinkage dependence on the location of clamps and pressure on the welded plate with thickness of 2.0 mm

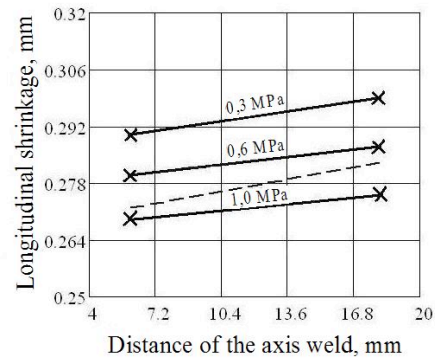


**Fig. 5.** Longitudinal shrinkage dependence on the location of clamps and pressure on the welded plate with thickness of 3.0 mm

machine. In Figs. 3-5 a linear dependence of the longitudinal shrinkage of the distance from the axis weld for different pressures of clamps on the welded plate is shown, where the solid line shows the results of numerical analyses and the dashed lines the results of three experiments with pressure clamps at 0.6 MPa at the distance of 6 mm and 18 mm from the axis weld respectively.

From Figs. 4 and 5 it can be seen that a pressure on the clamps of 0.6 MPa does not eliminate longitudinal slippage of samples with thickness 1.5 and 2.0 mm, as numerical analyses show, which is confirmed by experimental data with an error of less than 9,3%. Figs. 3-5 shows the change in the longitudinal shrinkage with the location of the clamps in relation to the axis weld. Thus an applied pressure of 1,0 MPa is insufficient for fixing and cannot guarantee the absence of slippage of a welded plate of thickness of 3.0 mm.

#### 4. Conclusions

1. Based on the thermal analysis of heat transfer in ANSYS / Multiphysics a thermal deformation numerical model was developed to assess the impact of the welding cycle of butt joints with copper backing to the residual strains of thin-sheet structures of austenitic corrosion-resistant steel with a thickness of 1.5 to 3.0 mm.
2. As a result of the numerical modeling of the stress-strain state of the samples it was established that when welding flat specimens with thickness of 3.0 mm on copper backing the distribution of residual strains for a given fixing pressure influences the width groove in the copper backing. By reducing the width of the groove from 8 to 6 mm the angular distortion is reduced from 1,04 ° to 0,8 ° for  $Q_{th} = 383$  kJ/m due to more intense heat transfer in the copper backing. The angular distortion of the welded plates when the slot width was changed from 8 to 6 mm remains the same for welding plates with thicknesses of 1.5 and 2.0 mm and welding parameters with  $Q_{th} = 156$  kJ/m and 234 kJ/m respectively.
3. The use of a numerical thermal deformation model allows to design welding machinery with minimal distortion of welded parts after welding and provides a significant increase in the efficiency of production.

---

## References

- [1] GOST 14771-76. *Gas-shielded arc welding. Welded joints. Main types, design elements and dimensions*. M.: Standart GOST, 1976. [In Russian]
- [2] Nikiforov R. [et al.] "Numerical simulation of penetration forms in tig welding consumable electrode to the copper lining", *Vestnik UGATU*, vol. 16, no.8, p. 89-93, 2012. [In Russian]
- [3] Nikiforov R. [et al.] "Determination the effect of heat transfer in copper plate to the melting of thin material during TIG-welding", *News Samara Scientific Center RAS*, vol. 14, no.2, p. 349-352, 2012. [in Russian]
- [4] G.A. Nikolaev, S.A. Kurkin, V.A. Vinokurov, *Welded constructions. The strength of welded joints and distortions of welded constructions: tutorial*. M.: Vshlola, 1982. [in Russian]
- [5] K.M. Ivanov. *Applied theory of plasticity: tutorial*. S.-Pet: Polytechnics, 2009. [in Russian]
- [6] V.G. Sorokin *Steels and alloys. Database: handbook*. M.: Internet Engeneering, 2003. [in Russian]
- [7] Chen B.-Q. *Prediction of Heating Induced Temperature Fields and Distortions in Steel Plates*: dissertation to obtain the degree of Master in Naval Architecture and Marine Engineering. Lisbon. 75 p., 2011.